oxidized and from calculations, to be highly sensitive to surface chemical functionality. Oxidized carbon is likely to show a greater variation in the O(2s) region than in many other oxygen-containing materials since the C(2s) energy is close to that of the O(2s) energy, and thus considerable mixing can occur between these two levels leading to significant chemical shifts. This situation is in contrast with the case of metal oxides where the O(2s) region is more corelike in its behavior.[20]

In general the valence-band region provides a more sensitive monitor of changes in surface chemistry than the core region. Thus changes in surface functionality result in significant differences (including in some cases separately resolved peaks) in the O(2s) region, as well as in the region at binding energies below 18 eV. In particular it can be seen that the calculations suggest that both the O(2s) binding energy and its separation from the C(2s) region provide analytical information allowing distinctions to be made regarding surface functionality. A striking example of the sensitivity of the valence-band region is in its predicted ability to distinguish between ether or epoxide type groups and hydroxide groups—groups that occur at a similar binding energy in the O(1s) core region. The valence-band region clearly has considerable potential as an analytical probe, one whose utility can be greatly assisted by accompanying calculations.

Acknowledgment. We are grateful to the Fibers Department of the Du Pont Co. for supporting this work and to the Department of Defense for providing funding for the X-ray diffraction equipment.

Registry No. Hydroquinone, 123-31-9; benzoquinone, 106-51-4; coronene, 191-07-1.

(20) Welsh, I. D.; Sherwood, P. M. A. *Phys. Rev. B* **1989**, *40*, 6386.

Semiconductor Particulate Films on Solid Supports

Xiao Kang Zhao and Janos H. Fendler*

Department of Chemistry, Syracuse University, Syracuse, New York 13244-4100

Received July 25, 1990

CdS and ZnS semiconductor particulate films, prepared in negatively charged monolayer interfaces and transferred to solid supports, have been characterized by reflectivity, absorption spectrophotometry, transmission electron microscopy, scanning tunneling microscopy, and electrical measurements. Incident-angle-dependent reflectivity measurements established the optical thicknesses of the semiconductor particulate films on solid supports to be only 5% smaller than those determined at the monolayer interfaces prior to their transfer. Absorption spectra of CdS and ZnS particulate films on quartz supports showed maxima around 239 and 200 nm and shoulders around 475 and 315 nm, respectively. Plots of absorbances at a given wavelength against thickness were linear for CdS and ZnS particulate films. Direct bandgaps for 63-, 125-, 163-, 204-, 263-, and 298-Å-thick CdS particulate films were evaluated to be 2.54, 2.48, 2.46, 2.44, 2.43, and 2.42 eV. Similarly, a direct bandgap of 3.75 eV was assessed for the 458-Å-thick ZnS particulate film. Heating of the CdS and ZnS films to 300–500 °C shifted the direct bandgaps to those corresponding to bulk semiconductors. Transmission electron micrographs of CdS films revealed the presence of CdS particles in a narrow size distribution with average diameters of 47 Å. The presence of 20–30-Å-thick, 40–50-Å-diameter CdS and 10–25-Å-thick, 30–40-Å-diameter ZnS particles in CdS and ZnS films were discerned by scanning tunneling microscopy. CdS films had dark resistivities of (3–6) × 10^7 Ω cm, which decreased upon illumination; they also developed photovoltages upon illumination. The action spectrum of the photoconductivity corresponded to the absorption spectrum of the CdS particulate film, indicating its origin to be the conduction band electrons and valence band holes produced in bandgap excitation.

Introduction

The altered mechanical, chemical, electrochemical, electrooptical, and magnetic properties that accompany size and dimensionality reductions have prompted the intensive investigation of nanosized particles and clusters.[1-3] In our laboratories, nanosized colloidal particles have been in situ generated and stabilized in such organized surfactant aggregates as reversed micelles,[4] surfactant and polymerized surfactant vesicles,[5-11] bilayer lipid membranes (BLMs),[12-14] and Langmuir–Blodgett (LB) films.[15,16] More recently, we reported that semiconductor particles could be in situ formed at monolayer interfaces. In particular, monolayers prepared from negatively charged arachidic acid (AA), bovine brain phosphatidylserine (PS), and *n*-hexadecyl-(4-vinylbenzamido)undecyl hydrogen phosphate (1) have been shown to attract cadmium and zinc ions and to act as templates for the in situ generation of semiconductor particles.[17] Controlled infusion of hydrogen sulfide resulted in the formation of covalent metal sulfide bonds at a large number of sites at

(1) Henglein, A. *Top. Curr. Chem.* **1988**, *143*, 113. Brus, L. A. *J. Phys. Chem.* **1986**, *90*, 2555. Andres, R. P.; Averback, R. S.; Brown, W. L.; Brus, L. E.; Goddard, W. A.; Kaldor, A.; Louie, S. G.; Moskovits, M.; Percy, P. S.; Riley, S. J.; Siegel, R. W.; Spaepen, F.; Wang, Y. *J. Mater. Res.* **1989**, *4*, 704.
(2) Henglein, A. *Chem. Rev.* **1989**, *89*, 1861.
(3) Fendler, J. H. *Chem. Rev.* **1987**, *87*, 877.
(4) Meyer, M.; Wallberg, C.: Kurihara, K.; Fendler, J. H. *J. Chem. Soc., Chem. Commun.* **1984**, 90.
(5) Youn, H. C.; Tricot, Y.-M.; Fendler, J. H. *J. Phys. Chem.* **1985**, *89*, 1236.
(6) Tricot, Y.-M.; Fendler, J. H. *J. Am. Chem. Soc.* **1984**, *106*, 2475.
(7) Tricot, Y.-M.; Fendler, J. H. *J. Am. Chem. Soc.* **1984**, *106*, 7359.
(8) Rafaeloff, R.; Tricot, Y.-M.; Nome, F.; Fendler, J. H. *J. Phys. Chem.* **1985**, *89*, 533.
(9) Rafaeloff, R.; Tricot, Y.-M.; Nome, F.; Tundo, P.; Fendler, J. H. *J. Phys. Chem.* **1985**, *89*, 1236.
(10) Tricot, Y.-M.; Emeren, Å.; Fendler, J. H. *J. Phys. Chem.* **1985**, *89*, 4721.
(11) Tricot, Y.-M.; Fendler, J. H. *J. Phys. Chem.* **1986**, *90*, 3369.
(12) Deleted in proof.
(13) Baral, S.; Fendler, J. H. *J. Am. Chem. Soc.* **1989**, *111*, 1604.
(14) Zhao, X. K.; Baral, S.; Fendler, J. H. *J. Phys. Chem.* **1990**, *94*, 2043.
(15) Xu, S.; Zhao, X. K.; Fendler, J. H. *Adv. Mater.* **1990**, *2*, 183.
(16) Yi, K. C.; Fendler, J. H. *Langmuir*, in press.
(17) Zhao, X. K.; Xu, S. Q.; Fendler, J. H. *Langmuir*, submitted for publication.

0897-4756/91/2803-0168$02.50/0

the compressed monolayer interface. The nascent metal sulfide microclusters grew laterally to linked, 30–50-Å diameter, 10–30-Å-thick polyparticulates. With continued infusion of H_2S, these polyparticles formed an interconnected semiconductor particulate film whose thickness grew to several hundred angstroms.[17]

Realization of the full potential of size-quantized semiconductor particles requires their transfer from an aqueous subphase to a solid support. Evidence is provided in this paper for the essentially intact transfer of monolayer-supported CdS and ZnS particles to solid substrates. Details are also given on the characterization of semiconductor particulate films by reflectivity, absorption spectrophotometry, transmission electron microscopy, scanning tunneling microscopy, and electrical measurements.

Experimental Section

Bovine brain phosphatidylserine (PS, Avanti Polar Lipids, Inc.), arachidic acid (AA, Sigma), dioctadecyldimethylammonium bromide (DODAB, Eastman), cadmium chloride, zinc chloride (Fisher), high-purity dry N_2 (Union Carbide), H_2S (Matheson), and spectroscopic grade chloroform (Aldrich) were used as received. Preparation and purification of polymerizable surfactants *n*-hexadecyl-11-(4-vinylbenzamido)undecyl hydrogen phosphate (1) and bis(2-(*n*-hexadecanoyloxy)ethyl)methyl(*p*-vinylbenzyl)-ammonium chloride (2) have been described.[18] Water was purified by a Millipore Milli-Q filter system provided with a 0.22-μm Millistack filter at the outlet.

The in situ generation of monolayer-supported semiconductor particles followed the described procedure.[17] Briefly, monolayers were compressed to their solid states by using a film balance enclosed in a Plexiglass hood. Injection of 200–250 μL of H_2S into the nitrogen-filled Plexiglass hood led to the slow development of semiconductor particles at the monolayer–metal ion interface.

The monolayer-supported semiconductor particulate film was transferred to solid substrates by horizontal lifting through the surface layers. Well-cleaned (chromic acid, dust-free water), 1.0 cm × 4.5 cm × 0.1 cm, spectroscopic-grade quartz plates, right-angle glass prisms, cellulose nitrate coated copper grids, highly oriented pyrolytic graphite (HOPG, Union Carbide, freshly cleaved), and glass slides or Teflon sheets (etched Cuflon, CF-A-01-5-5, Polyflon Corp.) were used as substrates for absorption spectrophotometry, reflectivity, transmission electron microscopy, scanning tunneling microscopy, and electrical measurements, respectively.

Absorption spectra were taken either on a Hewlett-Packard 8450 A diode-array spectrophotometer or on a PV 8800 Philips spectrophotometer.

Incident-angle-dependent reflectivities of the semiconductor particulate film were determined on a right-angle glass prism. A glass prism was tightly mounted on a precision rotating stage with the rotating axis in the vertical direction. Care was taken to provide good vibration isolation during measurements. The parallel polarized He–Ne laser light (13 mW, 6328 Å) was directed to the semiconductor film surface. The intensity of the incident light, corresponding to 100% reflectivity, was measured with $2\theta = 180°$. The intensity of the reflected light was measured by means of a Spectra Physics Model 404 silicon photocell power meter connected to a chart recorder.

Transmission electron micrographs were taken on a JEOL JEM-2000 EX 120-keV instrument. Samples were obtained on specially prepared substrates. Several pieces of 200-mesh copper grids were placed on a glass slide (1.0 cm × 4.5 cm × 0.1 cm) and immersed horizontally under the surface of purified water. A drop of cellulose nitrate (1.0% in amyl acetate, Ernest F. Fullam, Inc.) was allowed to spread evenly on the water surface. Subsequent to the formation of a thin, cellulose nitrate film, the glass slide carrying the copper grids was horizontally lifted through the cellulose nitrate coated water surface. Drying in a vacuum desiccator for a day produced the copper grid substrates used in transmission electron microscopic measurements.

Scanning tunneling microscopic images were acquired by means of an Angstrom Technology (Mesa, AZ) TAK 2.0 instrument operated in the constant-current mode. A Pt–Ir wire was used for the tunneling tip. Images were scanned with 5 lines/s and 0.5–1.0-V tip bias. Images were plotted on a CP 200U Mitsubishi color videocopy processor. Subsequent to transferring to graphite, the films were dried for 24 h, and surfactant monolayers were removed by gentle rinsing with $CHCl_3$ and ethanol. Eight separately prepared samples of CdS and ZnS were investigated. Images were taken in each sample in 50–100 different areas.

All electrical measurements were performed in a Faraday cage. Glass-supported semiconductor particulate films had two parallel gold or indium electrodes deposited in a 10^{-6}-Torr evaporator to 800-Å thickness prior or subsequent to the film transfer. Teflon-supported semiconductor particulate films had a copper (etched from cuflon prior to the film transfer) and a gold (or indium) electrode (vacuum deposited subsequent to the film transfer). Steady-state photovoltage and photoconductivity measurements were performed by connecting the electrodes to a Keithley Model 602 electrometer with an input impedance of 10^{14} Ω. Solid-supported particulate films were dried in a vacuum chamber (10^{-3} Torr) for 3 days prior to the electrical measurements. Samples were irradiated at a 45° angle by a 150-W xenon lamp via an ultraviolet sensitive optical fiber. Output from the electrometer was connected to a chart recorder. When needed, monochromatic light was provided by placing a Spex 1681, 0.22-m monochromator into the excitation light path. The energy per area (effected by the monochromatic light at a given wavelength) was determined by a Scientec 3652 energy/power meter.

Time-dependent photovoltage was investigated (also at 45° incident angle of irradiation) by using 10-ns 343-nm laser pulses (Lambda Physik EMG 101 MS excimer laser pumping a Lambda Physik 2002 dye laser, *p*-terphenyl). The two electrodes were directly connected to the input of a Tektronix 4662 storage oscilloscope in order to improve the response time. The oscilloscope scanning was synchronized with the laser pulse via a trigger and digital delay generator (Model 111 AR) with nanosecond accuracy. Photovoltage signals were transferred to a Zenith Data System computer (Z-100) via a programmable digitizer (Sony-Tektronix 390 AD). The instrument response time was 10^{-8} s. The energy of the laser pulse, varied by neutral density filters, was determined by means of a Scientec 3652 power/energy meter.

Temperature-dependent resistivities were determined by connecting the sample-covered substrate to a brass base. The brass was then heated bny an ac power supply via a heating wire. The temperature was measured by a point contact thermocouple.

Results and Discussion

Optical Thickness and Morphology of Semiconductor Particulate Films on Solid Supports. The uniform growth of semiconductor particles at the monolayer interface, ensured by the controlled and slow infusion of H_2S, was monitored by reflectivity measurements at $\theta = 10°$ incident angle.[17] With continuous slow H_2S infusion, the intensity of the light reflected from the monolayer-supported CdS film increased to a plateau value that corresponded to a limiting thickness of 300 ± 50 Å. A different behavior was found in the generation of ZnS particles. Sequential color changes, white → yellow → gold → orange → pink → violet → blue → green → yellow and gold, were accompanied by interference maxima and minima.[17] The effective refraction indexes, n_S, and volume fractions, F, of arachidate-monolayer-supported semiconductor particulate films are collected in Table I.

The monolayer-supported semiconductor particulate films were quite fragile. Vertical insertion of a stainless steel needle or a solid substrate caused a crack that grew to several centimeters in length. Traditional vertical Langmuir–Blodgett lifting could not be employed, therefore, for effecting transfer to solid substrates. In contrast, horizontal lifting of substrates resulting in the intact and quantitative deposition of the monolayer-supported, semiconductor particulate films. Any one of the 200–300-Å-

(18) Rolandi, R.; Paradiso, R.; Xu, S. Q.; Palmer, C.; Fendler, J. H. *J. Am. Chem. Soc.* **1989**, *111*, 5233.

Table I. Effective Refractive Indexes and Volume Fractions of Semiconductor Particulate Films at Monolayers and on Solid Supports[a]

	monolayer supported		solid supported		bulk semiconductor[b]
	n_s	F, %	n'_s	F', %	n_b
CdS	2.14	75.5	2.25	79.5	2.50
ZnS	1.84	55.4	1.88	58.3	2.37

[a] n_s = effective refractive index of the monolayer-supported semiconductor particulate film; n'_s = effective refractive index of the substrate-supported semiconductor particulate film; F = volume fraction of the monolayer-supported semiconductor particulate film; F' = volume fraction of the substrate-supported semiconductor particulate film. [b] Taken from ref 22.

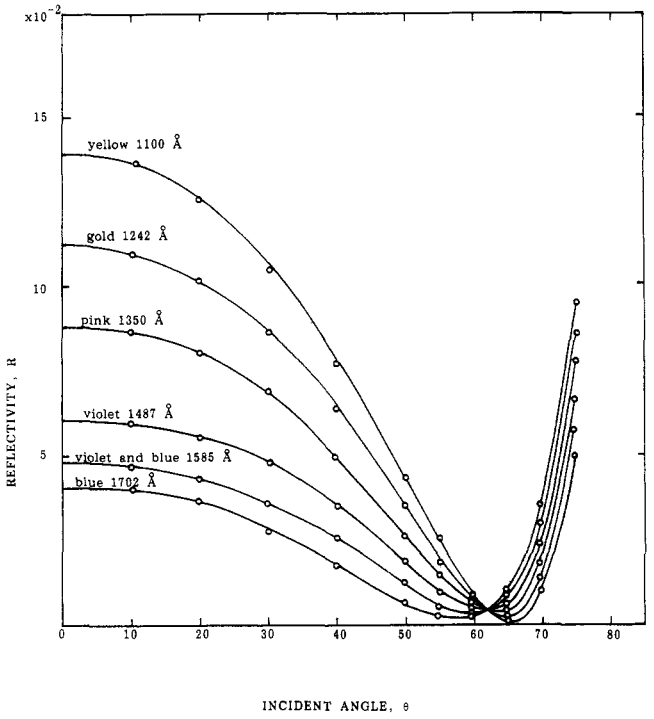

Figure 1. Incident-angle-dependent reflectivities of ZnS particulate films on glass prisms. The different curves were taken at different times subsequent to the beginning of H_2S infusion onto the zinc arachidate monolayers. The colors and calculated thicknesses are indicated on the curves. The intersection of the curves, 62.0°, defines the Brewster angle, θ_B.

thick CdS and 200–2000-Å-thick ZnS films appeared to be uniform and remained stable even on 200-mesh copper grids. Conversely, ZnS films thicker than 2000 Å cracked on drying.

Incident-angle-dependent reflectivities of differently colored ZnS particulate films on glass prisms (to obviate substrate interference), prepared by exposing zinc arachidate monolayers to H_2S for increasingly longer amounts of time, are shown in Figure 1. The intersection of the curves in Figure 1 defined the Brewster angle, $\theta_B = 62.0°$, which allowed the assessment of the effective refractive index, n'_S,[19] from

$$n'_S = \tan \theta_B \quad (1)$$

to be 1.88. This, in turn, permitted the numerical evaluation of the optical thicknesses of the semiconductor particulate films on the glass prism, d'_S, from the measured

(19) The primes (d'_S, n'_S, n'_S, n'_3, and F') refer to monolayer-coated semiconductor particulate films on *solid substrates* to distinguish them from the corresponding values determined in situ on aqueous surfaces (d_S, n_S, n, n_3, and F) in the work described in ref 17.

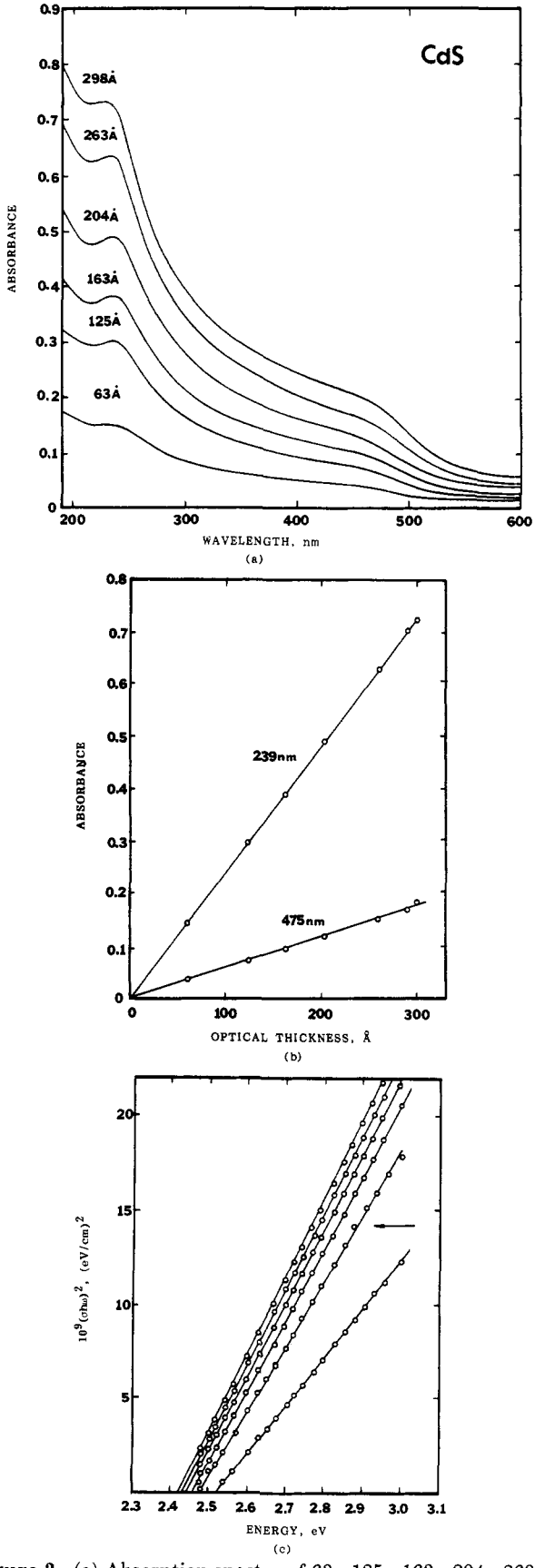

Figure 2. (a) Absorption spectra of 63-, 125-, 163-, 204-, 263-, and 298-Å-thick CdS particulate films on quartz substrates. The particulate films were prepared by the infusion of H_2S onto cadmium arachidate monolayers. (b) Plots of absorbances (A) against thicknesses (d'_S) of the CdS particulate film at 239 and 475 nm, according to eq 10. (c) Plots of $(\sigma h\omega)^2$ against energy (according to eq 11) for 63-, 125-, 163-, 204-, 263-, and 298-Å-thick (in the order shown by the arrow) CdS particulate films.

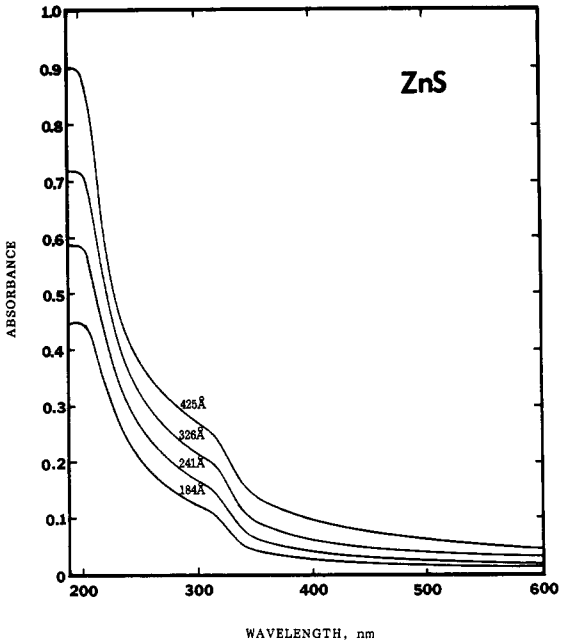

Figure 3. Absorption spectra of 184-, 241-, 326-, and 425-Å-thick ZnS particulate films on quartz substrates. The particulate films were prepared by the infusion of H_2S onto zinc arachidate monolayers.

reflectivities, R, by analogy with a four-phase system (air–monolayer–semiconductor particulate film–supporting solid substrate):

$$R = \frac{|r_{01}|^2 + |r_1|^2 + 2|r_{01}||r_1| \cos(\delta_{01} - \delta_2 + 2\beta_1)}{1 + |r_{01}|^2|r_1|^2 + 2|r_{01}||r_1| \cos(\delta_{01} + \delta_2 - 2\beta_1)} \quad (2)$$

$$r_1 = |r_1|e^{-i\delta_2} = \frac{r_{12} + r_{23}e^{-2i\beta_2}}{1 + r_{12}r_{23}e^{-2i\beta_2}} \quad (3)$$

$$\beta_1 = (2\pi d_1 n_1 \cos\theta_1)/\lambda \quad (4)$$

$$\beta_2 = (2\pi d'_S n'_S \cos\theta_S)/\lambda \quad (5)$$

r_{01}, r_{12}, and r_{23} are defined[20] as the Fresnel reflection coefficients (p-polarized light) at the air–monolayer, the monolayer–semiconductor particulate film, and the semiconductor particulate–substrate interfaces, respectively; n_1, n'_S, and n_3 as the refractive indexes of the monolayer, the particulate semiconductor film, and the glass substrate; d_1 and d'_S as the optical thicknesses of the monolayer and the particulate semiconductor film; and δ_{01} as the phase change at the air–monolayer interface. θ_1 and θ_S, the refraction angles of the monolayer and the semiconductor particulate film, respectively, are given by

$$n'_S \cos\theta_S = (n'^2_S - \sin^2\theta)^{1/2} \quad (6)$$

$$n_1 \cos\theta_1 = (n_1^2 - \sin^2\theta)^{1/2} \quad (7)$$

where θ is the angle of incidence. Substituting $n_1 = 1.52$ (AA), $n'_S = 1.88$, $n_3 = 1.52$ (glass), $d_1 = 26.7$ Å, and the measured reflectivity values (R) into eqs 2–7, the optical thicknesses of the six-colored, solid-supported ZnS films were calculated to be 1100, 1242, 1350, 1487, 1585, and 1702 Å (see Figure 1). These optical thicknesses, d'_S, were some 5% smaller than those determined for the corresponding monolayer-supported ZnS films, d_S (i.e., $d'_S/d_S = 0.95$). Reflectivity measurements provide strong evidence, therefore, for the essentially intact transfer of the monolayer-supported semiconductor particulate films to solid support by horizontal lifting.

(20) Zhao, X. K.; Xu, S.; Fendler, J. H. *J. Phys. Chem.* **1989**, *89*, 1861.

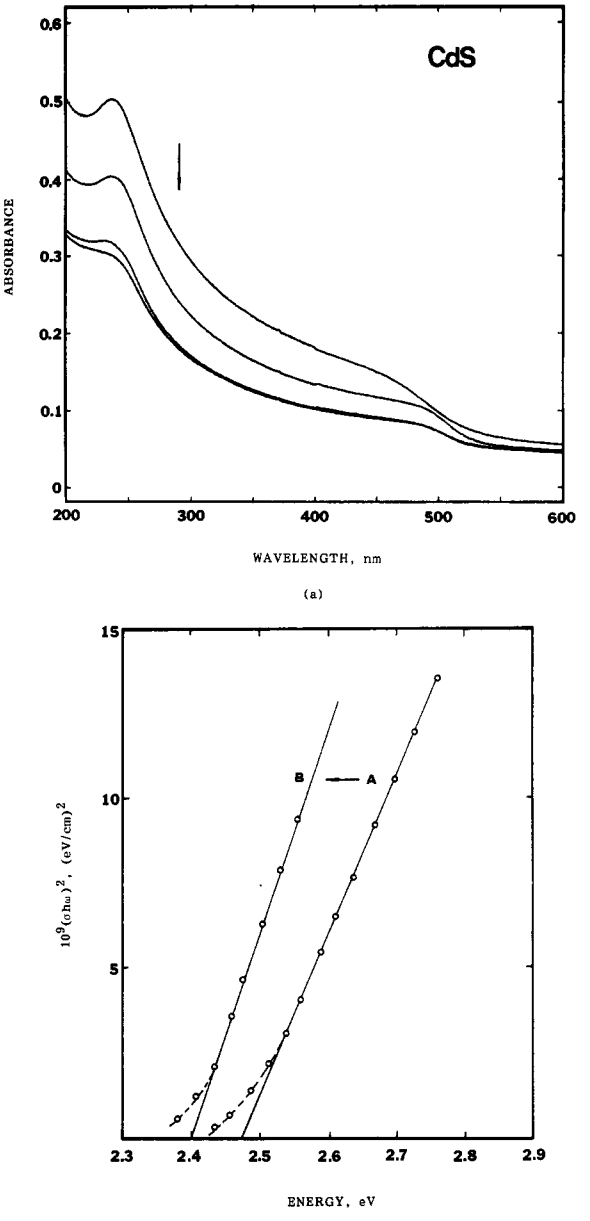

Figure 4. (a) Absorption spectra of a 192-Å-thick CdS particulate film on quartz substrate heated at 490 °C for 0, 5, 15, and 25 min (sequentially as indicated by the arrow). The particulate film was prepared by the infusion of H_2S onto a cadmium arachidate monolayer. (b) Plot of $(\sigma h\omega)^2$ against energy (eq 11) prior (curve A) and 5 min subsequent (curve B) to heating at 490 °C.

The effective refractive index of the host, n_h (i.e., the medium filling the space between the particles), for the solid-supported particulate film, was obtained by means of the Maxwell–Garnett approximation[21]

$$\frac{n'^2_S - n_h^2}{n'^2_S + 2n_h^2} = F'\frac{n_b^2 - n_h^2}{n_b^2 + 2n_h^2} \quad (8)$$

where n_b is the refractive index of the bulk semiconductor and F' is the volume fraction of the solid-supported film related to those assessed for the monolayer-supported film, F, by

$$F' = Fd_S/d'_S \quad (9)$$

Substituting $n'_S = 1.88$, $d'_S/d_S = 0.95$, $F = 55.4\%$, and n_b

(21) Garnett, M. S. C. *Philos, Trans. R. Soc. (London) A* **1904**, *203*, 385. Garnett, M. S. *Philos. Trans. R. Soc. (London) A* **1906**, *205*, 247.

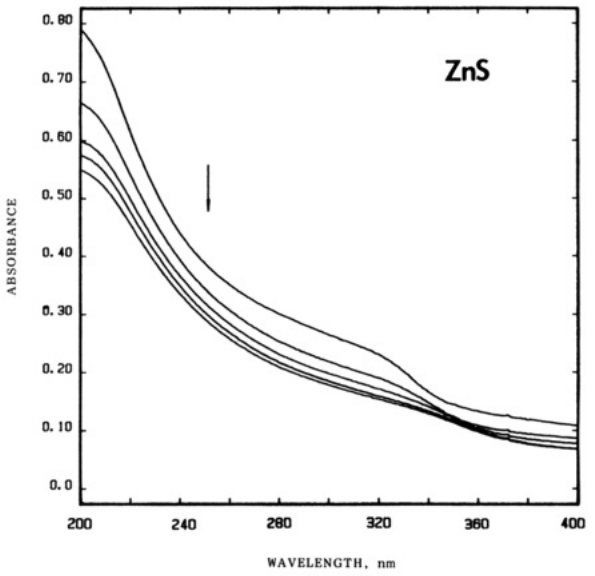

(a)

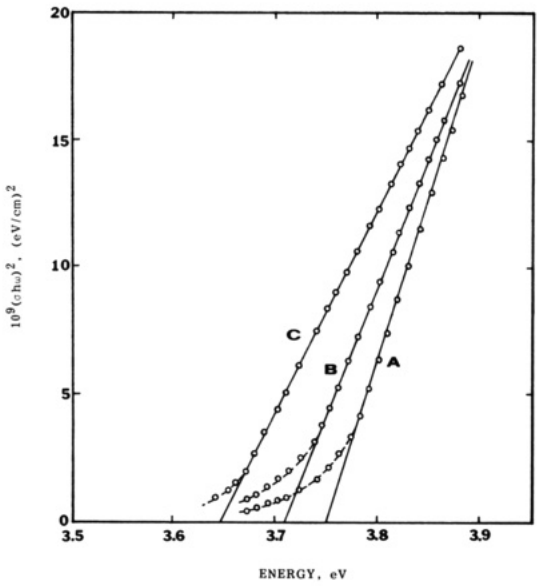

(b)

Figure 5. (a) Absorption spectra of a 359-Å-thick ZnS particulate film on quartz substrates heated at 300 °C for 0, 5, 15, 20, and 25 min (sequentially, as indicated by the arrow). The particulate film was prepared by the infusion of H_2S onto a zinc arachidate monolayer. (b) Plot of $(\sigma h\omega)^2$ against energy (eq 11) prior (curve A), 5 min (curve B), and 15 min subsequent (curve C) to heating at 300 °C.

= 2.37[22] into eqs 7 and 8, the refractive index of the host, n_h, for the solid-supported ZnS semiconductor particulate film was calculated to be 1.3. This value is quite similar to that of the aqueous subphase ($ZnCl_2$), indicating that a substantial amount of water is retained in the semiconductor particulate film, even after air drying. Similar behavior was found for CdS. The monolayer-supported CdS particulate film (F = 75.5%) was more compact than its ZnS counterpart (F = 55.4%). No porosity decrease was observed when a solid-supported film was air dried for 4 h. Drying in a vacuum chamber (10^{-3} Torr) for 24 h at ambient temperatures changed the optical thickness of a CdS particulate film from d_S = 155 Å to d'_S = 147 Å

(22) *Landolt-Bernstein New Series*; Springer: Berlin, 1983; Vol. 111, 17f, p 45. *Handbook of Chemistry and Physics*, 63rd ed.; CRC Press: Boca Raton, FL, 1982/1983; p B-165.

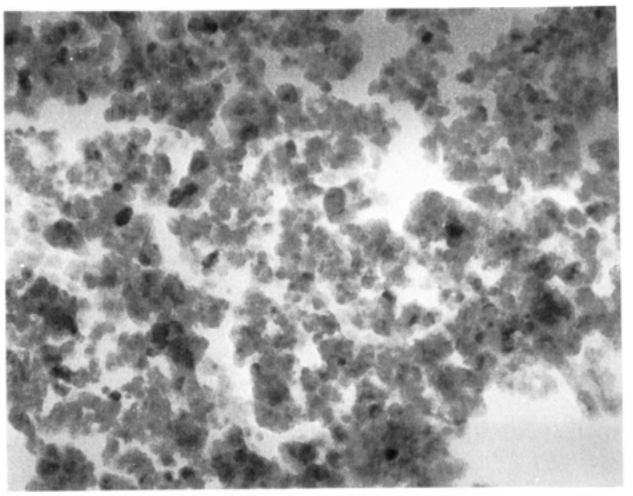

(a)

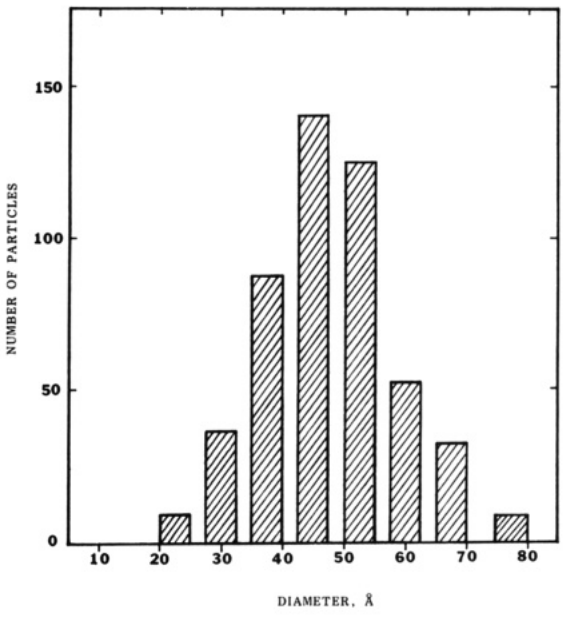

(b)

Figure 6. (a) Transmission electron micrographs of CdS particulate films on 200-mesh celluloid nitrate coated copper grids. The particulate film was prepared by the infusion of H_2S on cadmium arachidate monolayers. The bar indicates a distance of 500 Å. (b) Size distribution of the CdS particles, determined from transmission electron micrographs.

and the effective refractive index from n_S = 2.14 to n'_S = 2.25 (Table I).

Absorption Spectra of Semiconductor Particulate Films on Solid Supports. Absorption spectra of CdS and ZnS particulate films on quartz substrates (Figures 2 and 3) are quite similar to those published for the corresponding semiconductor particles.[1,2]

The absorption spectrum of a 63-Å-thick, CdS particulate film had a maximum at 239 nm, a shoulder at 460 nm, and an absorption edge at 488 nm (Figure 2). Increasing the thickness of the CdS particulate film manifested in a modest change in the appearance of the absorption spectrum. In particular, the absorption maximum became somewhat more pronounced and, along with the shoulder and absorption edge, red-shifted. Absorption spectra of ZnS films ($d_S \leq 500$ Å) on quartz supports showed a similar behavior (Figure 3).

Absorbances (A) increased linearly with increasing thicknesses of the CdS and ZnS particulate films (see

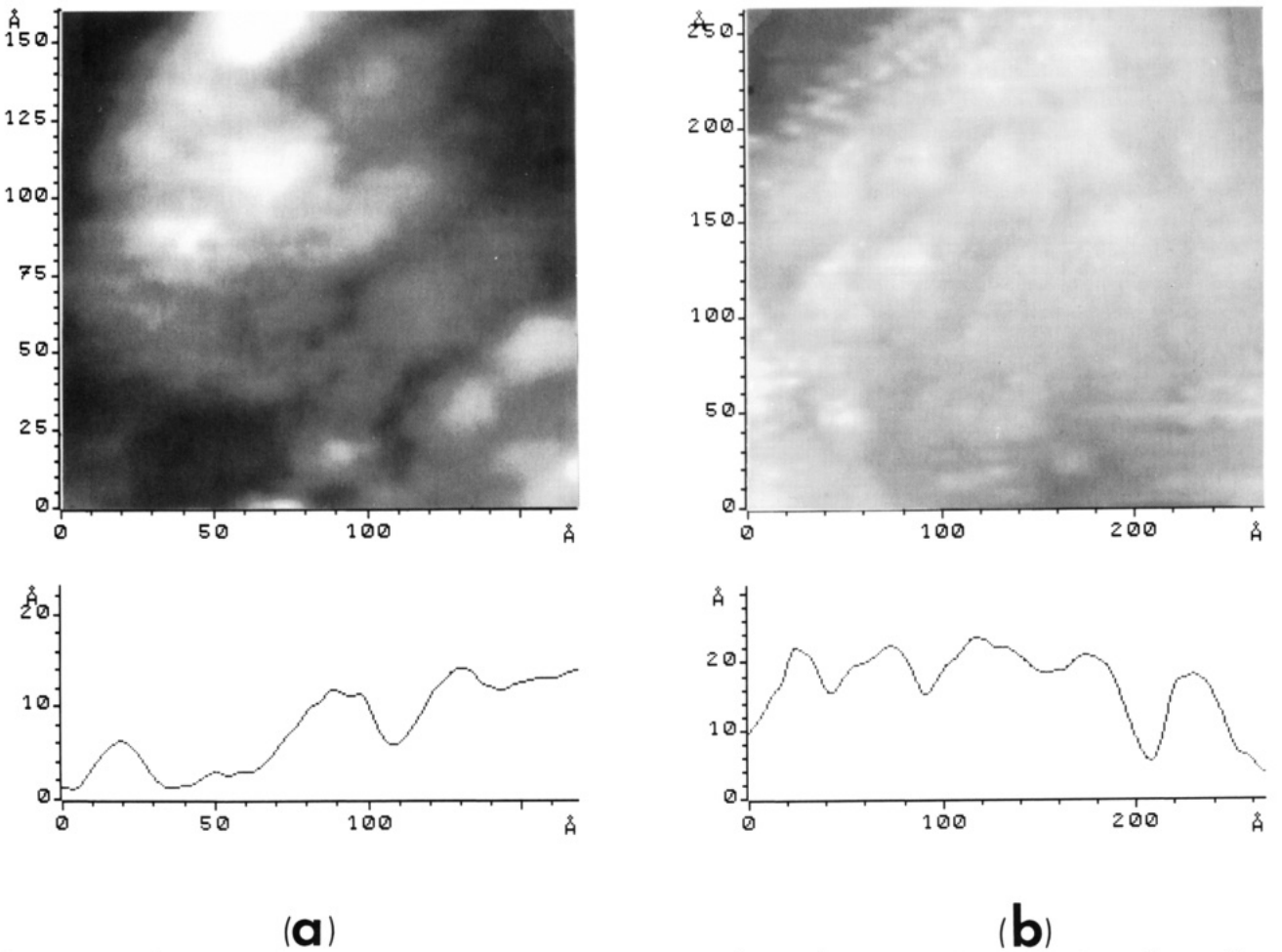

Figure 7. Two-dimensional STM images of HOPG-supported ZnS (a, 160 Å × 160 Å area scanned) and CdS (b, 270 Å × 270 Å area scanned) particulate films. Vertical dimensions are shown under the STM images. The particulate films were prepared by the infusion of H_2S to zinc and cadmium arachidate monolayers, respectively.

Figures 2a and 3). Absorption coefficients, σ, were calculated from

$$\sigma = A/d'_S \tag{10}$$

Absorption coefficients of 2.4×10^5 cm^{-1} at 239 nm and 5.8×10^4 cm^{-1} at 475 nm were obtained for the CdS particulate film (Figure 2b). This absorption coefficient agreed well with that determined for electrodeposited CdS films (σ(435 nm) = 2.06×10^4 cm^{-1}).[23] Similarly, an absorption coefficient at 5.8×10^4 cm^{-1} at 315 nm was determined for the ZnS particulate film. Knowledge of absorption coefficients allowed the assessment of direct bandgap energies, E_g, from

$$(\sigma h\omega)^2 = (h\omega - E_g)C \tag{11}$$

where $h\omega$ is the photon energy. Typical plots of the data, according to eq 11, are shown in Figure 2c. Values of E_g for CdS particulate films of d'_S = 63, 125, 163, 204, and 298 Å were assessed to be 2.54, 2.48, 2.46, 2.44, 2.43, and 2.42 eV (Figure 2c). Taking advantage of Henglein's published E_g vs particle-size curve,[2] we estimate the average diameter of the 63-Å-thick CdS particles to be ca. 50 Å. Increasing the thickness of the CdS particulate film resulted in progressively decreased direct bandgaps and, hence, in progressively larger CdS particles. At the thickest CdS particulate film, the measured CdS direct bandgap corresponded to that reported for bulk CdS semiconductors (2.4 eV).[2] A direct bandgap of 3.75 eV was assessed for the 359-Å-thick ZnS particulate film.

Prolonged heating of the semiconductor particulate films at high temperatures resulted in pronounced changes in their absorption spectra. The absorbance of a 192-Å-thick CdS particulate film (vacuum dried at 10^{-3} Torr for 3 days) decreased upon heating at 490 °C for 5, 15, and 25 min (Figure 4a). Five minutes of heating shifted the direct bandgap from 2.47 to 2.40 eV (or to an absorption edge of 515 nm) which was attributable to bulk CdS[2] (compare curve A with curve B in Figure 4b). A similar behavior was noted for 359-Å-thick ZnS particulate films (Figure 5); heating at 300 °C for 15 min shifted the direct bandgap from 3.75 to 3.64 eV (or to an absorption edge of 340 nm). Ignoring the weak absorption tails in Figures 4b and 5b results in an uncertainty of ca. 5%.[24] Prolonged heating of semiconductor particulate films have, therefore, two important consequences. First, their properties become similar to those found for bulk semiconductors. Second, they are annealed. Prolonged heating annealed the semiconductor particulate film to the substrate. Annealed semiconductor particulate films could not be washed or wiped away from their substrates. In contrast, vertical dipping of untreated semiconductor particulate films into water resulted in a partial loss of material from the subphase.

Transmission Electron Microscopy and Scanning Tunneling Microscopy of Semiconductor Particulate

(23) Preusser, S.; Cocivera, M. *Sol. Energy Mater.* **1990**, *20*, 1.

(24) Wang, Y.; Suna, A.; Mahler, W.; Kasowksi, R. *J. Chem. Phys.* **1987**, *87*, 7315.

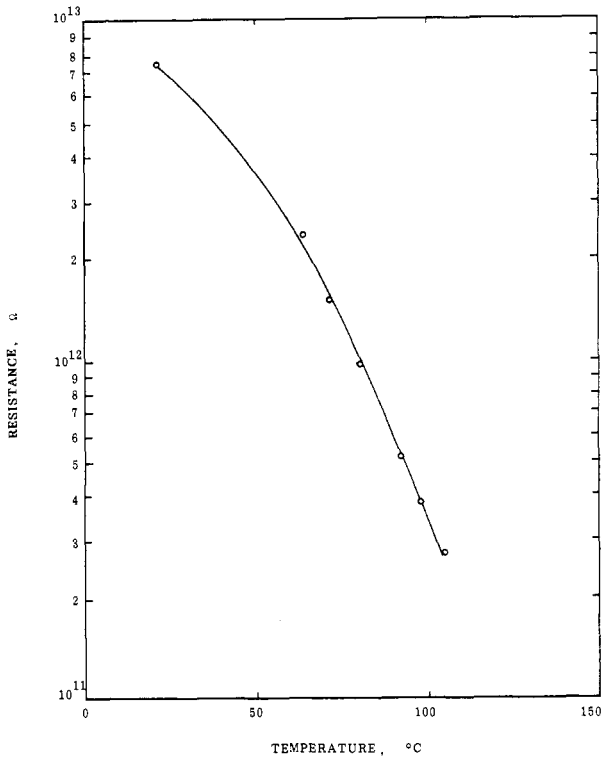

Figure 8. Plot of dark resistance of a 298-Å-thick CdS particulate film against temperature.

Films on Solid Supports. Transmission electron micrographs of 30–50-Å-thick, CdS particulate films indicated the presence of 20–80-Å-diameter particles in a relatively narrow size distribution with an average diameter of 47 Å (Figure 6). STM established HOPG to provide an atomically flat surface with periodic roughnesses on the order of 1 Å. Two-dimensional STM images of HOPG-supported ZnS and CdS particulate films are shown in Figure 7. The presence of 10–20-Å thick, 30–40-Å-diameter ZnS and 20–30-Å-thick, 40–50-Å diameter CdS particles are clearly discernible (see cross sections in the STM images in the lower parts of Figure 7). The widths of the semiconductor particles observed by STM (see peak-to-peak half-height widths in the lower parts of Figure 7) agree well with the corresponding diameters determined by transmission electron microscopy (Figure 6).

Electrical and Photoelectrical Properties of Semiconductor Particulate Films on Solid Supports. Electrical and photoelectrical measurements were carried out on CdS particulate films deposited on glass substrates or Teflon sheets. The resistivity (ρ) of a semiconductor particulate film, measured between two parallel copper electrodes, is given by

$$\rho = RLd'_S/a \qquad (12)$$

where R is the measured resistivity in ohms, L is the length of the copper electrodes, a is the distance between them, and d'_S is the thickness of the semiconductor particulate film. Resistivities of 200–300-Å-thick, CdS particulate films were determined to be (3–6) $\times 10^7$ Ω cm. The range represents measurements of 10 samples of different thicknesses and is due in part to the presence of different amounts of water in the films. The ρ values determined for CdS particulate films are some 6 orders of magnitude higher than those observed for materials having intrinsic conductivity.

The dark resistance of CdS particulate films was found to decrease with increasing temperature exponentially (Figure 8). Illumination decreased the resistivity (i.e., increased the conductivity) of CdS particulate films by some 2 orders of magnitude (Figure 9) and matched the absorption spectrum of the corresponding CdS particulate film nicely (Figure 9). Photoconductivity originates, therefore, in the production of conduction band electrons, e^-_{CB}, and valence band holes, h^+_{VB}, in bandgap irradiation of CdS:

$$CdS \xrightarrow{h\nu} e^-_{CB} + h^+_{VB} \qquad (13)$$

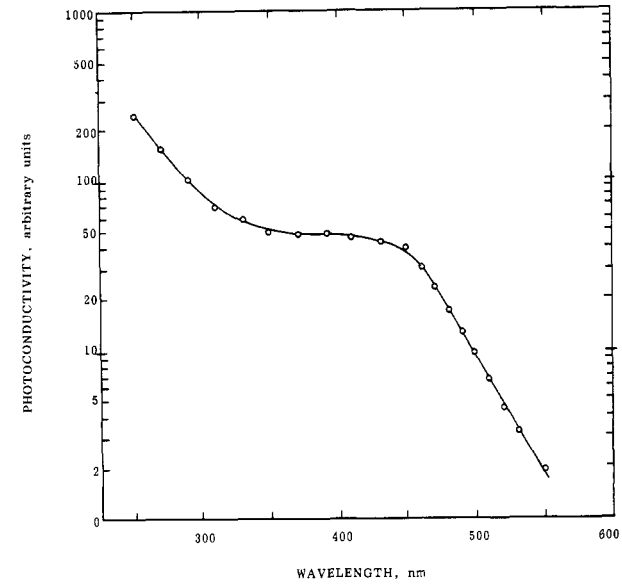

Figure 9. Photoconductivity action spectra of a 300-Å-thick CdS particulate film.

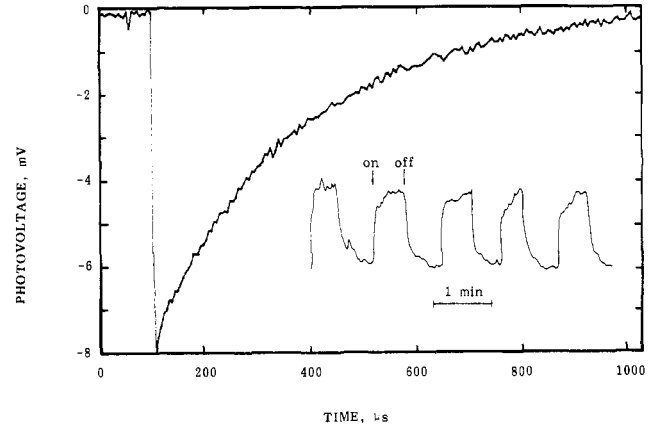

Figure 10. Transient and steady-state (insert) photovoltages of a 300-Å-thick CdS particulate film. Steady-state irradiation was performed by a 150-W xenon lamp. Transient photovoltage was generated by irradiation by a 10-ns 343-nm 1.0-mJ laser pulse.

Steady-state irradiation of CdS particulate films also resulted in the development of photovoltage (insert in Figure 10). Irradiation by a 10-ns 343-nm laser pulse gave rise to a transient photovoltage (Figure 10). The magnitude of the photovoltage (1–8 mV) was found to increase linearly with the energy of the laser pulse (0.1–1.0 mJ). The rise time of the transient signal, corresponding to eq 13, was faster than the response time of the instrument used (10 ns). The decay time of the signal was on the order of 3×10^{-4} s. This decay corresponds to charge recombination.

Acknowledgment. Support of this research by a grant from the Department of Energy is gratefully acknowledged.

Registry No. CdS, 1306-23-6; ZnS, 1314-98-3.